

This is the peer reviewed version of the following article:

A Chronology of Ancient Earthquake Damage in the Modena Cathedral (Italy): Integrated Dating of Mortars (14C, Pollen Record) and Bricks (TL) / Tirelli, Giulia; Bosi, Giovanna; Galli, Anna; Hajdas, Irka; Lindroos, Alf; Martini, Marco; Maspero, Francesco; Mazzanti, Marta; Olsen, Jesper; Panzeri, Laura; Ringbom, Åsa; Sibilio, Emanuela; Silvestri, Elena; Torri, Paola; Lugli, Stefano. - In: INTERNATIONAL JOURNAL OF ARCHITECTURAL HERITAGE. - ISSN 1558-3058. - 17:2(2023), pp. 326-342. [10.1080/15583058.2021.1922783]

Terms of use:

The terms and conditions for the reuse of this version of the manuscript are specified in the publishing policy. For all terms of use and more information see the publisher's website.

08/01/2026 15:03

Tirelli G., Bosi G., Galli A., Hajdas I., Lindroos A., Martini M., Maspero F., Mazzanti M., Olsen J., Panzeri L., Ringbom Å., Sibilis E., Silvestri E., Torri P., Lugli S., 2021, A chronology of ancient earthquake damage in the Modena cathedral (Italy): integrated dating of mortars (^{14}C , OSL, pollen record) and bricks (TL). *International Journal of Architectural Heritage*, 1-18.

A chronology of ancient earthquake damage in the Modena cathedral (Italy): integrated dating of mortars (^{14}C , pollen record) and bricks (TL)

Giulia Tirelli¹, Giovanna Bosi², Anna Galli^{3,5}, Irka Hajdas⁶, Alf Lindroos⁷, Marco Martini³, Francesco Maspero³, Marta Mazzanti², Jesper Olsen⁸, Laura Panzeri³, Åsa Ringbom⁹, Emanuela Sibilis^{3,4}, Elena Silvestri¹⁰, Paola Torri², Stefano Lugli¹

1 Department of Chemical and Geological Sciences, University of Modena and Reggio Emilia, Via Campi 103, 41125 Modena, Italy. giulia.tirelli@outlook.it, stefano.lugli@unimore.it

2 Laboratory of Palinology and Palaeobotany, Department of Life Sciences, University of Modena and Reggio Emilia, via Campi 287, 41125 Modena, Italy. giovanna.bosi@unimore.it, marta.mazzanti@unimore.it, paola.torri@unimore.it

3 Department of Materials Science, University of Milan – Bicocca, via Cozzi 55, 20125 Milano, Italy. anna.galli@unimib.it, m.martini@unimib.it, francesco.maspero@unimib.it, laura.panzeri@unimib.it, emanuela.sibilis@unimib.it,

5 CNR-IBFM, Via F.lli Cervi 93, 20090 Segrate (MI), Italy.

6 Laboratory of Ion Beam Physics, ETHZ, Otto-Stern-Weg 5, 8093 Zürich, Switzerland. hajdas@phys.ethz.ch

7 Faculty of Science and Engineering, Åbo Akademi University, Piispankatu 8, FI-20500 Turku, Finland. Alf.Lindroos@abo.fi

8 Aarhus AMS Centre, Department of Physics and Astronomy, University of Aarhus, DK-8000 Aarhus C, Denmark. jesper.olsen@phys.au.dk

9 Faculty of Arts, Psychology and Theology, Åbo Akademi University, Tehtaankatu 2, FI-20500, Turku, Finland. asa.ringbom@abo.fi

10 Studio Silvestri - Ingegneria e architettura, Viale Caduti in Guerra 35, 41121, Modena, Italy. elenasilvestri@studiotecnico-silvestri.it

Abstract

The 15th century cross-vaults of the medieval Modena Cathedral (UNESCO site) consist of intricate patches of different masonry portions bound by three types of lime mortars and at least two types of gypsum mortars. Such anomalous structure suggests multiple repair works over time after damaging earthquakes.

The absolute dating of lime mortars (^{14}C) and bricks (TL) integrated with the pollen record of mortars allowed to clarify the construction and restoration history of the vaults and to link the repairs to the earthquake chronology for the area. The results reveal that the original construction of the vaults (1404-1454) was carried out using lime mortar binding reused Roman and medieval older bricks. Lime mortar was used also for later repairs caused by earthquakes in the 16th and 17th centuries. Gypsum mortars were then used to entirely rebuild some vaults and to repair others in the 18th and 19th centuries.

The study indicates that unexpected damage could be revealed by the detailed chronology of masonry binders. These data represent fundamental steps to implement earthquake risk assessments and strengthening projects of ancient buildings.

Keywords: lime mortar dating, brick dating, gypsum mortar, earthquake damage, chronology, pollen

1. Introduction

In 2012 a seismic crisis struck the central Emilia Romagna region (northern Italy), strongly damaging the monumental heritage (Parisi and Augenti 2013). The medieval cathedral in Modena suffered significant damage, as brick fragments fell to the ground from the cross vaults (Baraccani et al. 2017). The vaults were a 15th century addition to the original 12th century structure of the cathedral. A complex network of fractures cut the vaults, witness of previous earthquake damage, but their internal structure was hidden by a thick plaster on both sides. Our fallen fragments inspection revealed that some part of the masonry of the vaults were bound with the traditional lime binder, but others were bound with a gypsum mortar. As a strengthening project was planned to increase the safety level of the Cathedral, the plaster cover was removed and we performed the detailed survey of the 23 vaults. An unexpected scenario was revealed, most of the vaults showed a complex patchwork of juxtaposed lime and gypsum masonry, whereas others consisted only of gypsum (Tirelli et al., 2020). This complex situation prompted two main questions: 1) Was the use of different binders possibly a clue for much larger ancient damage than that shown by the fracture survey alone? And 2) was lime or gypsum the original binder used for the construction of 15th century vaults?

This paper reports the results of an integrated study based on independent dating techniques to define the repair phases of the cathedral. The aim was to explore the possible correlation of the main restoration works to the earthquake chronology. Radiocarbon dating was carried out to date lime mortars and thermo-luminescence (TL) to date bricks. As gypsum mortar is not directly datable using radiocarbon, we performed also pollen analyses to obtain an indirect indication of the construction timing suggested by the local vegetation record, which saw the introduction of new ornamental species in the late history of the city.

2. The Modena cathedral: construction, earthquakes and repairs

The Modena Medieval UNESCO World Heritage Site consists of the Cathedral and the Civic tower Ghirlandina, celebrated examples of Romanesque art (Fig.1A). The building of the monumental complex started in 1099, date of the Cathedral's foundation (Silvestri 2013; Lubritto et al. 2015), to 1319 when the construction of the Ghirlandina bell tower was completed (Piccinini 2009). The church and the tower are covered by an impressive variety of ornamental stones coming from the despoliation of Roman monuments (Lugli et al. 2009) and also a large part of the bricks forming the core structures were taken from ancient Roman buildings (Panzeri et al. 2019). The cathedral roof was modified in the 15th century with the addition of 23 cross-vaults (Fig.1 B). Indirect and fragmentary clues from documents describing building contracts, accounts and correspondence indicate that the vaults were constructed in different phases, from 1404 to 1454 (Baracchi 1993). The first vaults to be built were

the easternmost in the central nave (C1, from 1404 to 1415) and in the southern nave (S9, from 1404 to 1433) The last one was the westernmost in the central nave, next to the façade (1447?-1453; see table 3 for the complete chronology).

Ancient documents indicate that the cathedral suffered multiple damaging events, but the location and extent of the repairs is virtually unknown. The catalogue of Italian earthquakes (Rovida et al. 2019) reports a number of historical earthquakes that struck the area after the vaults construction. According to the estimated values of Peak Ground Acceleration (PGA) for the cathedral (Baraccani et al., 2014), the possible damaging earthquakes occurred in the years: 1474 (0.232 PGA), 1501 (0.187 PGA), 1505 (0.055 PGA), 1586 (0.091 PGA), 1660 (0.172 PGA), 1671 (0.129 PGA), 1811 (0.072 PGA), 1832 (PGA not calculated, but damage reported in unpublished document), 1850 (0.144 PGA) and 1873 (0.059 PGA). The 2012 earthquake reached a Peak Ground Acceleration of 0.04.

3. Materials and Methods

3.1. Vaults masonry survey

We performed a detailed survey of the extrados of the 23 vaults (Fig. 1C, Fig. 2) to map the presence of different mortars after the preliminary map reported in Tirelli et al. (2020). The vaults have been numbered starting from the apses according to the nave orientation (north, central and south). Vaults N1 and S1 were explored only through two small openings in the mortar cover.

3.2. Petrographic analysis

A total of 32 mortar samples (lime and gypsum) were collected for petrographic analyses. Thin sections were prepared by vacuum impregnation with epoxy resin. The petrographic parameters of mortars (aggregate/binder, aggregate size and sorting and porosity) were calculated from digital image analysis of thin sections taken under the optical microscope in transmitted light according to the method described by Middeldorf et al 2019. Three images for sample were photographed from 4.5x3.0 mm thin sections and evaluated using the program ImageJ. Only three samples (C2-3AM, N2-DM and S1-2M) were not processed by image analysis due to high sample fragmentation. The aggregate sand supply sources have been identified by petrographic composition according to Lugli et al. 2007.

3.3. Radiocarbon dating of lime mortars: sequential dissolution method

Six lime mortars from the vaults showing multiple repairs (C1, C2, C3, C5, N9) were prepared for radiocarbon dating following the sequential dissolution methodology (Lindroos et al. 2007, 2019; Heinemeier et al. 2010). The mortar samples were crushed and dry sieved using increasingly fine mesh widths ranging between 75-500 µm in order to separate the soft carbonate binder mineral dust from the harder limestone particles. The grain-size fraction <100 µm was subsequently wet sieved and the 46–75 µm grain-size fraction was isolated and dried for ¹⁴C dating. The alkalinity test with phenolphthalein dissolved in alcohol was performed on the coarser grain size fraction (301-500 µm) to assess the presence of calcium hydroxide, which would react with the modern CO₂ in the atmosphere, producing secondary calcite. For this reason, alkaline samples are rejected for AMS dating. The 46–75 µm grain-size fraction was observed with cathodoluminescence (CL) to identify possible contaminants sources (underburned limestone fragment and carbonate aggregate).

Dissolution was done in a vacuum system with 85% phosphoric acid at 0° poured on the sample powders. Several consecutive CO₂ fraction were liberated and collected at different stages of the dissolution process. To minimize the amount of CO₂ from slowly dissolving contaminant carbonates, the first fraction was collected within 10 s. The following fractions were isolated after reaction times listed in Table 1. The mortar samples C1-1M, C2-3M, C3-1M; C5-4M, C5-5M, N9-3M, were

analyzed in three CO₂ fractions. The vials containing CO₂ were analyzed at the AMS ¹⁴C Dating Centre of Aarhus University and at the AMS facility Laboratory of Ion Beam Physics ETH Zurich. The conventional ¹⁴C dates were calibrated using the OxCal 4.3 program (Bronk Ramsey 2017). All calibrated results are reported at the 95% confidence level (2 sigma).

3.4. TL dating of bricks

The thermoluminescence dating was performed on the same vaults selected for ¹⁴C dating, analyzing ten brick samples (C1-1L, C3-1L, C5-1L, C5-4L, C5-5L, C5-6L, C5-7L, N3-3AL, N9-1L, N9-3L). Only in one case (C1-1L) we could not sample and date the binding mortar due to restoration works. We used the fine-grain dating technique (Zimmerman, 1971), which requires a relatively small amount of sample. The samples were prepared under dim red light, and the polymineral fine grain fraction (1-8 µm) was deposited on stainless steel discs. The fine-grain fraction was obtained from a suspension of the sample powder in acetone, an ultrasonic bath being used to disperse coagulation. Grains in the size range of 1 to 8 µm were separated by settling time of 20 and 2 minutes, respectively, using a 60 mm column (Aitken, 1985). For the evaluation of the palaeodose, the TL Multiple Aliquot Additive Dose protocol (MAAD, Aitken, 1985) was applied. TL measurements were performed using a home-made system based on the photon counting technique with a photomultiplier tube (EMI 9235QB) coupled to a blue filter (Corning BG12). The samples were heated from room temperature to 480°C at 15°C s⁻¹. Artificial irradiations were carried out by a 1.85 GBq ⁹⁰Sr-⁹⁰Y beta source (dose-rate: 3.57 Gy min⁻¹) and a 37 MBq ²⁴¹Am alpha source (dose-rate: 14.8 Gy min⁻¹). The annual dose rate was directly evaluated from the measurement of the radioactivity of the samples and their surroundings. The ²³⁸U and ²³²Th concentrations were obtained by total alpha counting using ZnS (Ag) scintillator discs assuming a Th/U concentration ratio equal to 3.16 (Aitken, 1985). The contribution due to ⁴⁰K content was obtained from the total concentration of K measured by flame photometry. For the annual dose rate calculations, an amount of water corresponding to 20±5 % of saturation was assumed. The external dose rate was evaluated on site with an ionization chamber for environmental dosimetry, to avoid the problem of inhomogeneity of the building materials around the samples.

3.5. Pollen analysis

A total of 6 pollen samples (C5-6M, C5-7M, N3-3AM, N8-2M, S9-1M, S9-4M) were extracted from the masonry after carefully chiseling away the exposed surface to avoid contamination by present-day pollen rain. The external rim of the sample fragments were eliminated in the laboratory and the sample cores were treated for pollen extraction by sieving and heavy liquid separation according to van der Kaars et al. (2001) and Florenzano et al. (2012). *Lycopodium* tablets were added to calculate concentrations (p/g=pollen/gram). Pollen identification was performed under the optical microscope at 1000x magnification on permanent slides by means of reference pollen collection, keys and atlases (e.g. Moore et al. 1991; Reille 1992-1998).

4. Results

4.1. Map of the vaults mortars

The map of the 15th century vaults shows a patchwork of lime and gypsum mortars (Fig. 2). The complex juxtaposition of different mortars does not allow to distinguish the original construction portions from the later repairs just using cross-cutting relationships. The repair sequence is particularly intricate in the northern nave (vaults N7, N8 and N9) and for the western part of the central nave (C4 and C5), where at least two different gypsum mortars were identified (G1 and G2,

Fig. 1C). All the mortars in the southern vaults consist of gypsum, with the only exception of in the westernmost vault (S9), where a small portion of lime mortar is present.

It was not possible to map all the different types of lime mortars by visual inspection alone, because a discrimination can be done only by petrography and radiocarbon dating, as illustrated below.

4.2. Petrography of lime mortars

The lime-based mortar show frequent rounded underburned limestone fragments up to 5 mm, with common micritic reaction edges, which fade into the surrounding binder, and scarce lime lumps, typically a few millimeters in diameter or less. The aggregate consists of fluvial sand with the following composition: micritic limestone fragments, sparry calcite, monocrystalline and polycrystalline quartz, k-feldspar, plagioclase, siltstone fragments, fossil fragments, serpentinite fragments, biotite, iron oxide and/or hydroxide grains. Six samples also present abundant bricks fragments (*cocciopesto*). No calcite neomorphism was observed in any of the samples. The mortars were classified in four groups based on the aggregate grain size, the aggregate binder ratio and sand provenance (Table 2).

Group 1 (C2-3M, C2-3AM, C3-1M, C5-1M, C5-4M, C5-5M) shows an aggregate binder ratio from 1.3 to 1.4 and is the only mortar containing *cocciopesto*. The aggregate is fine-grained, with grain size up to 5 mm across. The sand provenance is from the Panaro River (Fig. 3A, Table 2).

Group 2 (C1-1M, N1-1M, N1-2M, N2-2DM, N2-2FM, N7-3M, S1-1M, S1-2M, S9-4M) has an aggregate binder ratio from 1.1 to 1.5 and a high content of underburned limestone fragments. The aggregate grain size is from very fine to medium sand, moderately sorted, and was supplied from the Panaro River (Fig. 3B, Table 2).

Group 3 is characterized by lime mortars with an aggregate binder ratio from 2.1 to 2.2 and contains frequent underburned fragments (N5-1M, N8-1M, N9-3M). The aggregate grain size is from fine to medium sand, moderately sorted. The sand provenance is from the Panaro River (Fig. 3C, Table 2).

Group 4 (samples C1-4AM, C4-1AM and N3-2AM) consists of the lime plaster coating the upper side of the vaults. The aggregate binder ratio is from 2 to 2.1, the aggregate is well sorted and no underburned limestone fragments are present. The aggregate grain size is from fine to medium sand and the provenance is from the Secchia River (Fig. 3D, Table 2).

4.3. Petrography of gypsum mortars

Two different types gypsum mortar (G1 and G2) were identified by cross-cutting relationships and masonry texture (Fig. 3E, sample C5-6M, gypsum mortar G1, and sample C5-7M, gypsum mortar G2, Fig. 3F, Table 2). They are characterized by a binder of microcrystalline gypsum containing a few deformed selenite crystal fragments. Other components are fragments of carbonate rock and shale. The two mortars show different grain size and porosity: mortar G1 includes larger selenite crystal fragments, up to 3,5 mm across, and higher porosity with large rounded pores, whereas mortar G2 contains abundant fragment of micritic carbonate rocks. Anhydrite crystals are also present as result of the high temperature firing of gypsum in the kiln areas adjacent to the burning fuel. Mortar G2 was identified only in the central vaults C4 and C5. The attribution to the G1 mortar group of the vaults in the southern nave was done by visual inspection for the presence of large selenite fragments.

4.4. Radiocarbon dating of lime mortars

The results of the alkalinity test show a low alkalinity for all samples, indicating that they are suitable to be dated. The cathodoluminescence inspection confirmed the presence of older carbonate contaminants seen under the optical microscope.

The ^{14}C measurements with the hydrolysis data are presented in Table 1. The dating results are evaluated from the ^{14}C profiles of figure 5 and are interpreted in Table 3. The majority of the profiles

displays a concave curvature, or increasing slope (Lichtenberger et al. 2015), due to the rapid dissolution of the mortar binder and the slow onset of dissolution of the contaminants (Fig. 4A, C, E, G, I), see the discussion paragraph.

The ^{14}C age of CO_2 fraction 1 (590 ± 24 BP) for sample C1-1M corresponds to a calibrated calendar age of 1302-1368 (69.2 %) and 1382-1411 (26.2 %, Fig. 4B).

For sample C2-3M the first two CO_2 fractions agree within the given error margins and contamination can be ruled out (criterion I, Heinemeier et al. 2010; Ringbom et al. 2011; Lindroos et al. 2018). The combined calibration of fraction 1 and 2 yields a ^{14}C age of 492 ± 24 BP corresponding to a calibrated calendar age of 1409-1445 (Fig. 4D).

Sample C3-1M.1 provided a low CO_2 pressure value for fraction 1 and the hydrolysis was performed a second time in order to obtain a larger CO_2 volume (sample C3-1M.2.1). This fraction yielded ^{14}C ages of 506 ± 26 BP corresponding to a calibrated calendar age of 1399-1445 (Fig. 4F).

The results of sample C5-4M dating were rejected because the ^{14}C profile shows a decreasing slope (Fig. 4M). In this case, it was not possible to read the binder age from the profile (Fig. 4N).

The radiocarbon age of fraction 1 for sample C5-5M is 508 ± 34 BP, calibrated to 1325-1345 (7.4%) and 1393-1449 (88.0%; Fig. 4H)

The ^{14}C age of the fraction 1 (534 ± 35 BP) of sample N9-3M corresponds to a calibrated calendar age 1315-1356 (28.1%) and 1388-1441 (67.3%), which coincides with the expected age for the original construction (1433-1454) (Fig. 4L).

4.5. TL dating of bricks

The TL dating results, listed in Table 3, show that most of the bricks yielded ages different from the original construction time span. Only one sample shows a 15th century age (vault C3: 1500 ± 60), all the other sample are either older or younger. TL dates range in age from the Roman period (vault C5 in both lime and gypsum mortar, 225 ± 170 and 250 ± 170), the 13th century (vault C5, 1280 ± 65), the 14th century (vault C5, 1320 ± 65 and vault N9, 1330 ± 75 and 1340 ± 70), the 15th-16th century (vault C3, 1500 ± 60), the 17th century (vault C1, 1640 ± 40) to the 19th century (vault C5, 1835 ± 20 and vault N3, 1820 ± 20 and 1840 ± 20).

4.6. Pollen in lime and gypsum mortars

The state of pollen preservation is good, concentration is low, from about 1000 to just over 2000 np/g, as reported for other mortars (Langgut et al. 2013). A total of 108 taxa were identified in the mortar samples and their association and environmental significance will be given elsewhere. Here we report the taxa relevant (Fig. 5) for dating purpose as chronological markers, such as “exotic” ornamental trees of recent introduction and plants that were extensively cultivated in particular historic periods in the area. These taxa are: 1) *Ginkgo biloba* in samples N3-3AM and N8-2M; 2) *Ailanthus altissima* in sample N8-2M; 3) *Cedrus* in sample N3-3AM and 3) *Cannabis sativa* (hemp) discovered in 5 samples (C5-6M, C5-7M, N3-3AM, S9-1M, S9-4M). Pollen concentration of taxa is always $<1\%$, except for hemp, which has a range from 0.4 to 6.2%.

5. Discussion

5.1. Mortar composition

In the 50 years' time span of the vault construction inferred from documents (1404-1454), group 2 mortar appears to have been used to build the older vaults, whereas the younger vaults were built using group 1 and 3 mortars (Table 3). The only lime repair that we have discovered was manufactured using the mortar of group 3. It follows that the identified mortar groups have no chronological significance, but probably reflect the various contractors that worked on the vault

construction and later repairs using their own preparation techniques and raw materials in various phases.

The variable aggregate grain size may be due to collection of sand in the Panaro river from distinct sedimentation areas, such as meander bars, longitudinal bars or terraces and in different time periods of the year, during the flood (spring and fall) or the dry seasons (summer and winter). Sands from the Panaro river were also used as aggregate for the construction of the apses (mortar A and B of Caroselli et al., in press).

The lack of underburned fragments in group 4 suggests a relatively recent, semi-industrial, lime preparation technique, possibly dating to a 19th century intervention designed to protect the fractured vaults with a thick lime mortar cover. Aggregate sand supplied from the Secchia river started to be used in the cathedral only since the 13th century modifications (Caroselli et al., in press). The use of gypsum mortars in the rebuilding and in the repairs of the cathedral vaults represents an unexpected, unique case. In the area the use of gypsum as binder started only from the second half of the 17th century (Lugli 2019) when the famous *scagliola* artworks from Carpi (Modena) and the *stucco* decorations typical of the baroque art became very popular. Gypsum mortar in brick masonries was normally used for very limited repairs and not for structural elements.

The reason why the ecclesiastical authority decided to switch from lime to gypsum mortar is unknown. Gypsum mortar would have been less expensive in terms of: 1) fuel consumption, as lower temperatures are required for firing gypsum (105 °C) than lime (in excess of 800°C) and 2) preparation technique, as gypsum does not need to be mixed with a sand aggregate because of its expansion properties upon hydration. Gypsum mortars are also lighter and provide faster setting time than lime mortars. The carbonate and shale fragments observed within the gypsum groundmass are not added elements, but derive from the selenite raw rock used to prepare the mortars (Fig. 3F, Lugli et al., 2010).

Unfortunately, gypsum mortars cannot be directly dated, and in some cases the reuse of bricks older than the vaults construction time does not allow to pinpoint the timing of the repairs (see below). The cross-cutting relationships indicate that gypsum mortar G1 predates G2 (Fig. 1).

5.2. Radiocarbon dating

The Modena cathedral lime mortars represent one of the most challenging case for radiocarbon dating. This is because the mortars are rich in incompletely burned limestone fragments and the sand aggregate consists of 33.7-43.3 % of carbonate grains (Panaro river, Lugli et al. 2007). These components represent potential contaminants, possibly leading to older ages than the construction time. But the advantage of the sequential dissolution method is that the dead carbon influence is revealed by the shape of the ^{14}C profile, as contaminants dissolve at a slower pace than the binder and their effect is negligible in the first collected CO_2 fraction (fraction 1, Lindroos et al. 2018).

The *cocciopesto*-rich mortars (group 1) could also provide biased results because they contain less dateable carbonate, are less permeable to atmospheric CO_2 and may harden very slowly. They may also contain uncarbonated calcium hydroxide, which could capture modern ^{14}C providing younger ages than the actual construction time (Lindroos et al. 2011; Ringbom et al. 2011, 2014; Michalska et al. 2017; Lindroos et al. 2020). In our case, only one sample was affected by the problem, as revealed by the decreasing slope of the ^{14}C profile demonstrating delayed hardening (C5-4M, Fig. 4M).

All the tested samples are in the range of the vaults construction time, although a slight influence of dead carbon contamination may have caused steep ^{14}C profiles and a minor shift towards older ages for the initial CO_2 fractions, (Fig. 4). These results highlight the good potential for the sequential dissolution method to recognize and reduce to the minimum the contamination effect, even for the worst-case scenarios given by high dead carbon from underburned fragments and carbonate aggregate, and the delayed carbonation effect induced by *cocciopesto*.

5.3. TL dating

The results of the thermoluminescence dating of brick indicate several repairs carried out using bricks produced in the 17th, 18th and 19th centuries (Table 3). Some of the restoration works also extensively reused bricks manufactured before the construction of the vaults, in the 12th and 14th century, and even ancient Roman bricks. The reuse of older bricks was documented for the medieval core structure of the tower and the cathedral (Panzeri et al. 2019), but was not known for the late additions, such as the 15th century vaults. Ancient documents attest that the original construction works were often halted because of the lack of building materials (Baracchi 1987). Ornamental stones and bricks were available only when buried roman monuments were discovered and exploited (see discussion in Lugli et al., in press). As a general rule, the reuse of older bricks could have been a common practice in the earlier repair phases (16th to 17th centuries), although we cannot exclude that bricks coming from demolition of older (medieval) buildings, were also used also for the 18th and 19th century repairs.

5.4 Pollen record

The pollen spectra record plants from the areas nearby the city center trapped during the laying and setting of the mortars. Ginkgo tree (*Ginkgo biloba* L.) arrived in Italy (Padua, Milan and Pisa) in the second half of the 18th century (Targioni Tozzetti 1853; Saccardo 1909; Maniero 2000) and its fortune as ornamental plant was rather quick, becoming widely cultivated throughout Europe in the mid-19th century (Crane et al. 2013).

Tree of Heaven (*Ailanthus altissima* (Mill.) Swingle) also arrived in Italy in the mid-18th century and by the mid-19th century it appears widespread and perfectly naturalized in some areas, becoming a highly invasive species (Saccardo 1909; Maniero 2000; Pignatti et al. 2017-2019).

These two marker plants, *Ginkgo* and *Ailanthus*, are listed in the oldest *Index Plantarum* of the Modena Botanical Garden (Fabriani 1811), which is located not far from the cathedral, and therefore the taxa are witnesses of the urban area at least from the beginning of the 19th century.

The species of the genus *Cedrus* (*C. libani* A. Rich., *C. deodara* [D. Don.] G. Don, *C. atlantica* [Endl.] Manetti ex Carrière - not distinguishable with pollen) seem to arrive in Italy between the mid-18th and the mid-19th century (Saccardo 1909; Maniero 2000), immediately becoming popular ornamental plants (Pignatti et al. 2017-2019).

Hemp (*Cannabis sativa*) cultivation started in the area since the Bronze Age (Mercuri et al. 2006) and grew continuously through the Middle Age to the beginning of the 19th and 20th century (Venturi & Amaducci 1999, Casalgrandi 2018), but does not appear in the present-day pollen rain in town (Mercuri et al. 2001). The relatively high concentration seen in samples S9-1M and C5-7M (up to 6.2 %) requires rather extensive field cultivation, setting the age of these two mortars to repairs conducted in the second half of the 19th century (Table 3 and Fig 6).

5.5. The chronology of vault construction and repairs

The concomitant presence of lime and gypsum binder in the mortars of some vaults and the exclusive presence of gypsum in others clearly points to multiple repair phases, which led also to the complete reconstruction of some vaults using at least two different gypsum binders. Such extensive works could only have been triggered by severe damage caused by earthquakes. The possible damaging earthquakes may be identified comparing the time lines given by the ¹⁴C and TL chronological data (Table 3) coupled with the pollen spectra interpretation, as illustrated in figure 6.

Radiocarbon dating demonstrates that lime mortar was the original vault construction binder from 1404 to 1454. This is also the case for the southern nave, where only a small portion of original lime masonry (vault S9) survived the complete reconstruction of unknown timing with gypsum mortar.

Vault C1 was originally built using lime mortar and older bricks, and was subsequently partially reconstructed using lime mortar in the 17th century, possibly as a result of the 1660, 1671 earthquakes, as deduced by the brick dates.

Vaults C3 is the only one originally built with bricks produced at the time of the vault construction (15th century). The overlapping ^{14}C of the mortar and TL date of the bounded bricks allows to refine the construction time from 1440 to 1449, which matches the timing inferred by documents (1446-1447?).

Vault N8 represents the only case where lime mortar provided radiocarbon calendar ages that are younger (16th-17th century) than the original construction time. The vault was modified at least two times. A first restoration by lime mortar and re-used bricks was carried out immediately after the original construction, possibly as result of the 1501, 1505, 1586, 1660 or 1671 earthquakes. A second intervention was then probably triggered by the 1811 earthquake, as suggested by pollen content and brick dating record, or is the result of multiple repairs in the 18th and 19th century. New bricks were used for this second repair, kept together by a gypsum mortar.

Vault C5 was originally built using lime mortar and re-used bricks. At least two different restoration phases followed. A first partial reconstruction was carried out using gypsum mortar G1 and older bricks. A second intervention was performed using gypsum mortar G2 in the 19th century, probably to mend the damage caused by the 1811, 1832 or 1850 earthquakes.

Vault N3 was modified in the 19th century using gypsum mortar, possibly following the 1811, 1832 or 1850 earthquakes, as suggested by the brick dates and pollen record.

Vaults N9 and S9 were originally built using lime mortar and older bricks, whereas gypsum mortar was used for later repair with re-used bricks. Unfortunately, as for the previous vaults modified with gypsum mortar and re-used bricks, the timing of the later intervention could not be defined, but pollen markers found in vault S9 suggest possible late repairs after the 1850 or 1873 earthquakes.

These considerations indicate that lime mortar was rarely used for later repairs in favor of gypsum. Mortar gypsum G1 in the central and northern vaults dates to the 18th-19th century, whereas G2 was used in the 19th century, as revealed by brick dates. In the southern nave, mortar G1 could have been deployed even before the 18th century, but the large reuse of ancient brick prevented us to recognize when gypsum started to be preferred instead of lime for the repairs.

5. Conclusions

The complex structure of the 15th century vaults of the Modena cathedral consists of irregular patches of lime and gypsum mortars suggesting multiple repairs due to damaging earthquakes. The integrated chronology obtained by three independent dating methods has allowed to clarify the vaults construction and restoration history, assessing the extent of the damaged areas.

The sequential dissolution method provided reliable radiocarbon results for lime mortars matching the historic documents time span, despite the potential contamination by dead carbon due to the large presence of underburned limestone fragments and carbonate grains in the aggregate. The thermoluminescence of bricks demonstrated that the cathedral represents an unprecedented example of building material re-use even for the 15th century structural modifications.

The petrographic and absolute dating results revealed that different types of lime mortars were used both for the original construction of the vaults from 1404 to 1454 and for later repairs in the 16th and 17 centuries. At least two types of gypsum binder were subsequently used to repair some vaults in the 18th and 19th centuries. Other vaults were entirely rebuilt using gypsum mortar. The reasons and age of this unprecedented large use of gypsum binder for structural elements are unknown, but were possibly driven by construction cost. Several damaging seismic events were possibly responsible for the reparation works, which are not documented in the historical records.

The results of this multidisciplinary research highlight the possibility that unexpected and severe damage could be revealed by detailed binder chronology, which may add further information to implement earthquake risk assessment and structural strengthening projects. This is because crack

and fracture survey alone may reveal only the relatively recent damage pattern suffered by ancient buildings.

Acknowledgements

This work was supported financially by Capitolo metropolitano and Comune di Modena. We thank also Soprintendenza archeologia, belle arti e paesaggio per la città metropolitana di Bologna e le province di Modena, Reggio Emilia e Ferrara for the cooperation and support.

References

Aitken M. 1985. Thermoluminescence Dating. Oxford: Academic Press, pp.359.

Baraccani S., Silvestri S., Palermo M., Gasparini G., Trombetti T., Dib A. 2014. The assessment of the seismic behaviour of the cathedral of Modena, Italy. In proceedings of the Second European conference on earthquake engineering and seismology, Istanbul, Turkey, European Association for Earthquake Engineering (EAE), 6954-6965.

Baraccani S., Gasparini G., Palermo M., Silvestri S., Trombetti T. 2017. The structural behavior of the masonry vaults of the Cathedral of Modena. In Proceedings of the 5th International Conference on Architecture and Civil Engineering, Singapore, 8-9 May: https://doi.org/10.5176/2301-394X_ACE17.92

Baracchi O. 1987. La cattedrale di Modena nei documenti della fabbrica di San Geminiano In Atti e memorie della Deputazione di storia patria per le antiche provincie modenesi. 11 (9): 157-222.

Baracchi O. 1993. Volte a crociera e affreschi del Duomo: nuovi documenti del '400 e '500. In Atti e memorie della Deputazione di storia patria per le antiche provincie modenesi. 11 (15): 131-156.

Bronk Ramsey C. 2017. OxCal [WWW program] version 4.3. Oxford Radiocarbon Accelerator Unit: University of Oxford. Available at <https://c14.arch.ox.ac.uk/oxcal/OxCal>.

Caroselli M., Lugli S., Marchetti Dori S., Maiorano C., in press, Analisi petrografica delle malte e degli intonaci della cattedrale di Modena: contributo alla definizione delle fasi costruttive. Collana Contributi per la storia materiale del Duomo di Modena.

Casalgrandi G.L. 2018. Il libro della canapa. Il Fiorino, Modena.

Crane P.R., Nagata T., Mutara J., Ohi-Toma T., DuVal A., Nesbitt M., Jarvis C. 2013. Ginkgo biloba: connections with people and art across a thousand years. Curti's Botanical Magazine, 30 (3): 239-260. <https://doi.org/10.1111/curt.12040>

Fabriani G. 1811. Index Plantarum quae extant in Horto botanico Mutinensi, anno MDCCCXI. Eredi Soliani, Modena.

Florenzano A., Mercuri A.M., Pederzoli A., Torri P., Bosi G., Olmi L., Rinaldi R., Bandini Mazzanti M. 2012. The significance of intestinal parasite remains in pollen samples from medieval pits in the Piazza Garibaldi of Parma, Emilia Romagna, Northern Italy. Geoarcheology. 27: 34-47. <https://doi.org/10.1002/gea.21390>

- Heinemeier J., Ringbom Å., Lindroos A., Sveinbjörnsdóttir A.E. 2010. Successful AMS ^{14}C dating of non-hydraulic lime mortars from the Medieval churches of the Åland Islands, Finland. *Radiocarbon*. 52(1): 171-204. <https://doi.org/10.1017/S0033822200045124>
- Langgut D., Gadot Y., Porat N. Lipschits O. 2013. Fossil pollen reveals the secrets of the Royal Persian Garden at Ramat Rahel, Jerusalem. *Palynology*, 37 (1): 115-129. <https://doi.org/10.1080/01916122.2012.736418>
- Lichtenberger A., Lindroos A., Raja R., Heinemeier J. 2015. Radiocarbon analysis of mortar from Roman and Byzantine water management installations in the Northwest Quarter of Jerash, Jordan, *Journal of Archaeological Science. Reports* 2: 114–127. <https://doi.org/10.1016/j.jasrep.2015.01.001>
- Lindroos A., Heinemeier J., Ringbom Å., Braskén M., Sveinbjörnsdóttir Á. 2007. Mortar dating using AMS ^{14}C and sequential dissolution: examples from Medieval, non-hydraulic lime mortars from the Åland Islands, SW Finland. *Radiocarbon*. 49(1): 47-67. <https://doi.org/10.1017/S0033822200041898>
- Lindroos A., Heinemeier J., Ringbom Å., Brock F., Sonck-Koota P., Pehkonen M., Suksi J. 2011. Problems in radiocarbon dating of Roman pozzolana mortars. *Proceedings from Building Roma Aeterna, conference, Rome, March 23-2, 2008*. In Ringbom Å., Hohlfelder R. (eds). *Commentationes Humanarum Litterarum, Societas Scientiarum Fennica*. 128: 214–230.
- Lindroos A., Heinemeier J., Ringbom Å., Hodgins G., Sonck-Koota P., Sjöberg P., Lancaster L., Kaisti R., Brock F., Ranta H., Caroselli M., Lugli S. 2018. Radiocarbon dating historical mortars: lime lumps and/or binder carbonate? *Radiocarbon*. 60 (3): 875-899. <https://doi.org/10.1017/RDC.2018.17>
- Lindroos A., Heinemeier J., Ringbom Å. 2019. Radiocarbon dating of lime mortars. The sequential dissolution method. In Rita Vecchiattini. *Archeologia dell'Architettura*, vol.24. Sesto Fiorentino: All'Insegna del Giglio, p. 11-17.
- Lindroos A., Ringbom Å., Heinemeier J., Hajdas I., Olsen J. 2020. Delayed hardening and reactivation of binder calcite, common problems in radiocarbon dating of lime mortars. *Radiocarbon*: 1-13. <https://doi.org/10.1017/RDC.2020.5>
- Lubritto C., Caroselli M., Lugli S., Marzaioli F., Nonni S., Marchetti Dori S., Terrasi F. 2015. AMS radiocarbon dating of mortar. The case study of the medieval UNESCO site of Modena. *Nuclear Instruments and Methods in Physics Research B* 361:614–619. <https://doi.org/10.1016/j.nimb.2015.05.015>
- Lugli S., 2019, Il gesso in natura e nell'arte. *GeoArcheoGypsum2019*, *Geologia e archeologia del gesso: dal lapis specularis alla scagliola*, (Eds.) D. Gulli S. Lugli, R. Ruggieri, R. Ferlisi. Palermo, Regione siciliana, 17-31.
- Lugli, S., Marchetti Dori, S., Fontana D. 2007. Alluvial sand composition as a tool to unravel the Late Quaternary sedimentation of the Modena Plain, northern Italy. In Arribas J., Critelli S., Johnsson M.J. *Sedimentary Provenance and Petrogenesis: Perspectives from Petrography and Geochemistry*. United States: Geological Society of America Special Paper: 420, 57-72. [https://doi.org/10.1130/2006.2420\(05\)](https://doi.org/10.1130/2006.2420(05))
- Lugli S., Papazzoni C.A., Gavioli S., Melloni C., Rossetti G., Tintori S., Zanfognini R., 2009, The stones of the Ghirlandina tower. In “La Torre Ghirlandina un progetto per la conservazione”, R. Cadignani (Ed.), Luca Sossella Editore. 96-117.

- Lugli S., Manzi V., Roveri M., Schreiber B.C. 2010. The Primary Lower Gypsum in the Mediterranean: A new facies interpretation for the first stage of the Messinian salinity crisis. *Palaeogeography, Palaeoclimatology, Palaeoecology*, 297, 83-99.
- Lugli, S., Papazzoni, C.A., Rossetti, G., Tintori, S., in press. Il paramento lapideo del Duomo di Modena. *Collana Contributi per la storia materiale del Duomo di Modena*.
- Maniero F. 2000. *Fitocronologia d'Italia*. Firenze: Leo S. Olschki, pp. 296.
- Mercuri A.M., Massamba N'siala I., Barbieri G. 2001. 2000 Pollen Calendar-2 hourly Airborne Pollen Monitoring Station – University of Modena and Reggio Emilia (Botanical Garden/Geophysical Observatory). *Atti Soc. Nat. Mat. Modena*, 132: 25-64.
- Mercuri A.M., Accorsi C.A., Bandini Mazzanti M., Bosi G., Cardarelli A., Labate D., Marchesini M., Trevisan Grandi G. 2006. Economy and environment of Bronze Age settlements – Terramaras – in the Po Plain (Northern Italy): first results of the archaeobotanical research at the Terramara di Montale. *Vegetation History and Archaeobotany* 16: 43-60.
- Michalska D., Czernik J., Goslar T. 2017. Methodological Aspect of Mortars Dating (Poznań, Poland, MODIS). *Radiocarbon*. 59 (6): 1891-1906. <https://doi.org/10.1017/RDC.2017.128>
- Middendorf B., Schade T., Kraus K. 2019. Quantitative Analysis of Historic Mortars by Digital Image Analysis of Thin Sections. *Restoration of Buildings and Monuments*. 23: 83–92.
- Moore P.D., Webb J.A., Collins M.E. 1991. *Pollen Analysis*, II ediz. Blackwell Sc. Publ., Oxford.
- Panzeri L., Caroselli M., Galli A., Lugli S., Martini M., Sibilia E. 2019. Mortar OSL and brick TL dating: the case study of the UNESCO world heritage site of Modena. *Quaternary Geochronology*. 49: 236-241. <https://doi.org/10.1016/j.quageo.2018.03.005>
- Parisi F., Augenti N. 2013. Earthquake damages to cultural heritage constructions and simplified assessment of artworks. *Engineering Failure Analysis*. 34: 735–760. <https://doi.org/10.1016/j.engfailanal.2013.01.005>
- Piccinini F. 2009. Notes on the construction of the Cathedral and the Ghirlandina Tower. In Cadignani R. (ed) *The Ghirlandina Tower. Conservation Project*. Roma: Luca Sossella Editore: 42-47.
- Pignatti S., Guarino R., La Rosa M. 2017-2019. *Flora d'Italia* (2nd ed.). Edagricole, Bologna.
- Reille M. 1992. *Pollen et spores d'Europe et d'Afrique du Nord*. Laboratoire de botanique historique et palinologie. URA CNRS 1152, Marseille.
- Ringbom Å., Heinemeier J., Lindroos A., Brock F. 2011. Mortar dating and Roman Pozzolana, results and interpretation. In Ringbom Å., Hohlfelder R. (eds). *Proceedings from Building Roma Aeterna*, conference in Rome, March 23–25 2008. *Commentationes Humanarum Litterarum, Societas Scientiarum Fennica*. 128: 187–208.
- Ringbom Å., Lindroos A., Heinemeier J., Sonck-Koota P. 2014. 19 years of mortar dating: learning from experience. *Radiocarbon*. 56 (2): 619–635. <https://doi.org/10.2458/56.17469>

Rovida A., Locati M., Camassi R., Lolli B., Gasperini P. (eds), 2019. Italian Parametric Earthquake Catalogue (CPTI15), version 2.0. Istituto Nazionale di Geofisica e Vulcanologia (INGV). <https://doi.org/10.13127/CPTI/CPTI15.2>

Saccardo P.A. 1909. Cronologia della Flora italiana. Padova: Tipografia del Seminario, pp.390.

Silvestri E. 2013. Una rilettura delle fasi costruttive del Duomo di Modena. Atti e Memorie. Deputazione di Storia Patria per le Antiche Provincie Modenesi 11(35):117–149.

Targioni Tozzetti A. 1853. Cenni storici sulla introduzione di varie piante nell'agricoltura ed orticoltura Toscana. Tipografia Galileana, Firenze.

Tirelli G., Lugli S., Galli A., Hajdas I., Lindroos A., Martini M., Maspero F., Olsen J., Ringbom Å., Sibilà E., Caroselli M., Silvestri E., Panzeri L. 2020. Integrated dating of construction and restoration of the Modena cathedral vaults (northern Italy): preliminary results. Radiocarbon: 1-11. <https://doi.org/10.1017/RDC.2020.10>

Van der Kaars S., Penny D., Tibby J., Fluin J., Dam R., Suparan P. 2001. Late quaternary palaeoecology, palynology and palaeolimnology of a tropical lowland swamp: Rawa Danau, West Java, Indonesia. Palaeogeography, Palaeoclimatology, Palaeoecology. 171 (3-4):185-212. [https://doi.org/10.1016/S0031-0182\(01\)00245-0](https://doi.org/10.1016/S0031-0182(01)00245-0)

Venturi G., Amaducci M.T. 1999. Le colture da fibra. Edagricole, Bologna.

Zimmerman D.W. 1971. Thermoluminescent dating using fine grains from pottery. Archeometry. 13:29-52. <https://doi.org/10.1111/j.1475-4754.1971.tb00028.x>

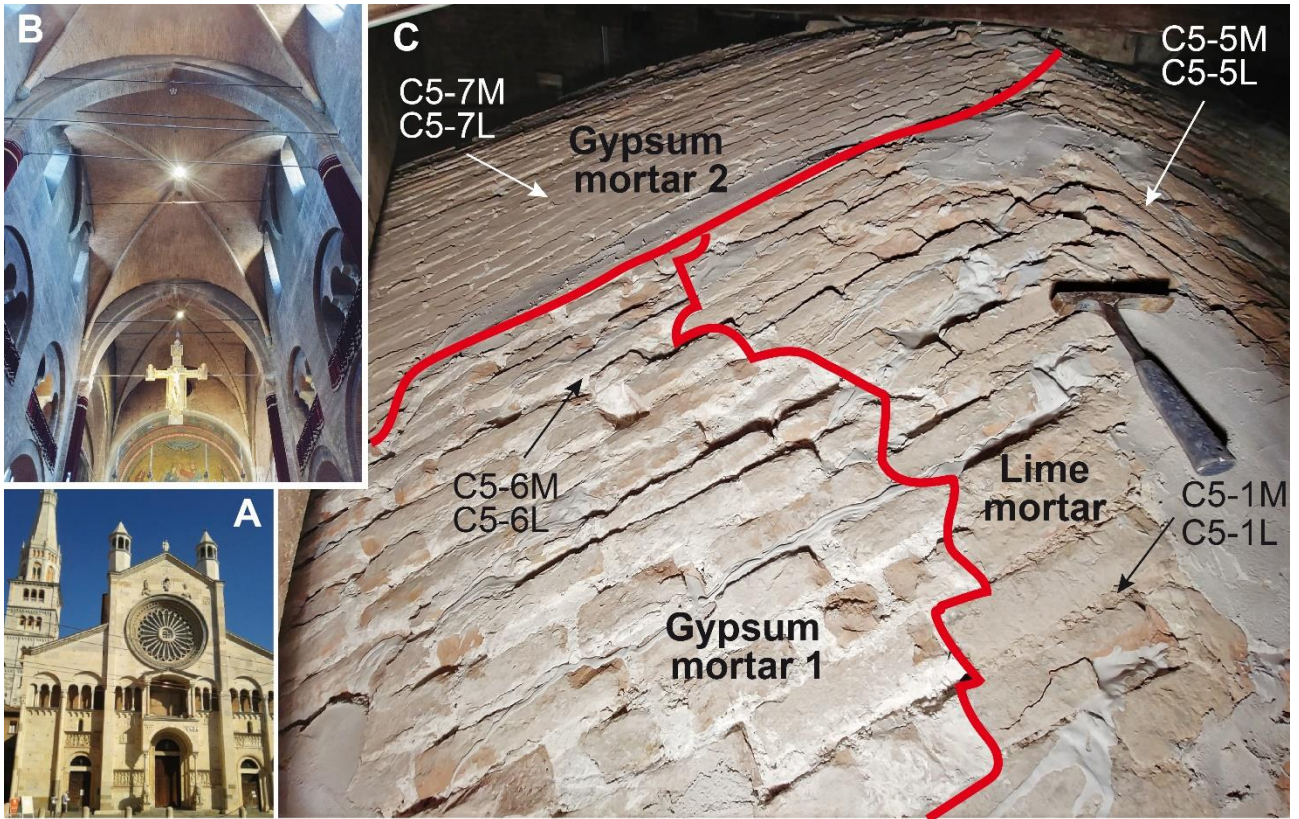


Fig. 1: A) The Modena cathedral façade and bell tower. B) View of the cathedral ceiling showing the intrados of vault C1 (in the background of the suspended cross), C2 (top center) and C3 (topmost side, partially visible); the lower part of the vaults is covered by a painted plaster reproducing a brick masonry texture. C) partial view of vault C5 extrados showing different masonry textures and mortars with the location of the analyzed samples. Rock hammer for scale.

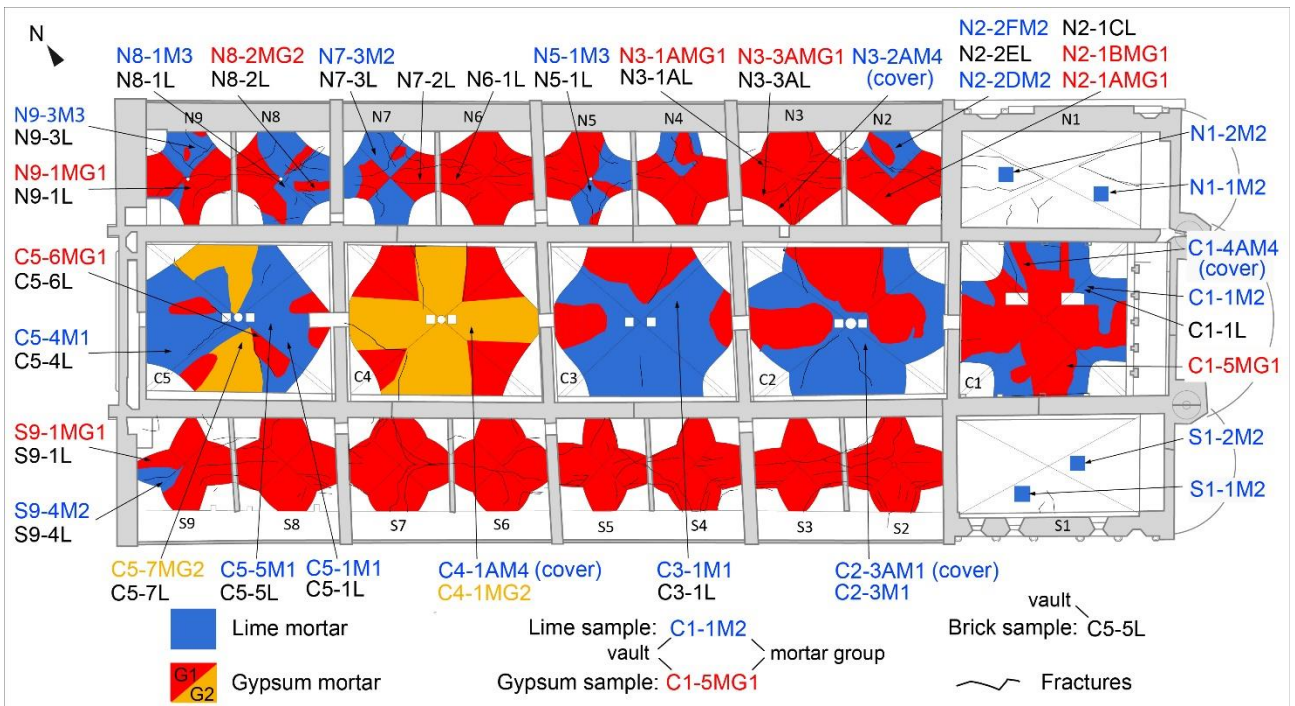


Fig. 2: Vaults extrados map of the Modena Cathedral lime and gypsum mortars. The samples location and the fracture network are also shown (modified from Tirelli et al., 2020).

Sample subsample / CO ₂ -fraction	Material	Grain size (μm)	Reaction time (s) from t ₀	Carbon yield (tot) (%)	Fraction size (relative 1)	¹⁴ C age (BP)	±	δ ¹³ C ‰ VPDB	Laboratory nr
C1-1M.1.1	Bulk mortar	46-75	6	3.40% C	0-0.09	590	24	-28,2	ETH-86835
C1-1M.1.2			17		0.09-0.24	816	23	-13,3	ETH-86829
C1-1M.1.3			110		0.24-0.45	2876	23	2,6	ETH-86830
C2-3M.1.1	Bulk mortar	46-75	7	5,69% C	0-0.10	516	34	-20,1	ETH-96989
C2-3M.1.2			17		0.10-0.25	471	32	-8,8	ETH-96990
C2-3M.1.3			70		0.25-0.41	589	31	-6,4	ETH-96991
C3-1M.1.1	Bulk mortar	46-75	6	2.53% C	0-0.12	593	27	-20,3	ETH-86836
C3-1M.1.2			30		0.12-0.37	645	23	-16,2	ETH-86932
C3-1M.1.3			120		0.37-0.62	1601	23	-8	ETH-86933
C3-1M.2.1	Bulk mortar	46-75	14	2.44% C	0-0.08	506	26	-23,8	ETH-86837
C5-4M.1.1	Bulk mortar	46-75	6	5.36% C	0-0.09	125	75	n.r.	ARR-25642.1
C5-4M.1.2			24		0.09-0.26	592	37	n.r.	ARR-25642.2
C5-4M.1.3			90		0.26-0.41	924	89	n.r.	ARR-25642.3
C5-5M.1.1	Bulk mortar	46-75	5	6,08% C	0-0.10	508	34	-19,8	ETH-96986
C5-5M.1.2			22		0.10-0.25	562	32	-10,3	ETH-96987
C5-5M.1.3			60		0.25-0.40	879	32	-8,6	ETH-96988
N9-3M.1.1	Bulk mortar	46-75	7	4.48% C	0-0.04	534	35	n.r.	AAR-25638.2
N9-3M.1.2			24		0.04-0.56	829	44	n.r.	AAR-25638.3
N9-3M.1.3			75		0.56-0.72	1773	35	n.r.	AAR-25638.1

carbon yield (tot) (%) = total carbon yield after about one hour of dissolution

n.r. = not reported

AAR = Aarhus AMS lab; ETH = ETH Zurich

Table 1 Hydrolysis data, ¹⁴C results and δ¹³C values for the dated samples.

Vault	Sample	Mortar composition	Mortar group	Aggregate/binder	Aggregate sand size and sorting	Aggregate provenance	Underburned limestone max size (mm)	Cocciopesto max size (mm)	Selenite max size (mm)	Porosity (%)	Pore max size (mm)
C1	C1-1M	lime	2	1.5	very fine-medium, moderately sorted	Panaro river	4.2	-	-	19.2	-
	C1-4AM	lime (cover)	4	2.1	fine-medium, well sorted	Secchia river	-	-	-	22.9	-
	C1-5M	gypsum	G1	-	-	-	-	-	2.4	4.7	1.0
C2	C2-3AM	lime (cover)	1	-	very fine-fine, poorly sorted	Panaro river	2.8	3.1	-	-	-
	C2-3M	lime	1	1.4	very fine-fine, poorly sorted	Panaro river	1.9	5.1	-	2.3	-
C3	C3-1M	lime	1	1.3	very fine-fine, moderately sorted	Panaro river	4.8	2.6	-	1.6	-
C4	C4-1AM	lime (cover)	4	2	fine-medium, well sorted	Secchia river	-	-	-	4.6	-
	C4-1M	gypsum	G2	-	-	-	-	-	1.6	3.0	0.5
C5	C5-1M	lime	1	1.4	very fine-fine, moderately sorted	Panaro river	3.8	5.4	-	3.8	-
	C5-4M	lime	1	1.3	very fine-fine, moderately sorted	Panaro river	2.3	3.3	-	4.5	-
	C5-5M	lime	1	1.4	very fine-fine, moderately sorted	Panaro river	4.5	5.2	-	4.3	-
	C5-6M	gypsum	G1	-	-	-	-	-	3.5	7.6	1.5
	C5-7M	gypsum	G2	-	-	-	-	-	1.8	3.1	0.6
N1	N1-1M	lime	2	1.5	very fine-medium, moderately sorted	Panaro river	5.1	-	-	8.4	-
	N1-2M	lime	2	1.5	very fine-medium, moderately sorted	Panaro river	5.6	-	-	5.1	-
N2	N2-1AM	gypsum	G1	-	-	-	-	-	3.2	4.7	0.8
	N2-1BM	gypsum	G1	-	-	-	-	-	1.3	4.6	0.6
	N2-2DM	lime	2	-	very fine-medium, moderately sorted	Panaro river	2.6	-	-	-	-
	N2-2FM	lime	2	1.5	very fine-medium, moderately sorted	Panaro river	5.2	-	-	19.5	-
N3	N3-1AM	gypsum	G1	-	-	-	-	-	1.0	6.2	1.1
	N3-2AM	lime (cover)	4	2	fine-medium, well sorted	Secchia river	-	-	-	8.8	-
	N3-3AM	gypsum	G1	-	-	-	-	-	3.2	7.5	1.2
N5	N5-1M	lime	3	2.1	fine-medium, moderately sorted	Panaro river	3.9	-	-	11.7	-
N7	N7-3M	lime	2	1.1	very fine-fine, well sorted	Panaro river	3.3	-	-	5.6	-
N8	N8-1M Tirelli et al. 2020	lime	3	2.2	fine-medium, moderately sorted	Panaro river	3.8	-	-	4.9	-
	N8-2M	gypsum	G1	-	-	-	-	-	1.3	6.1	1.5
N9	N9-1M	gypsum	G1	-	-	-	-	-	2.7	6.5	1.4
	N9-3M	lime	3	2.2	fine-medium, moderately sorted	Panaro river	3.7	-	-	8.2	-
S1	S1-1M	lime	2	1.5	very fine-medium, poorly sorted	Panaro river	5.3	-	-	8.3	-
	S1-2M	lime	2	-	very fine-medium, poorly sorted	Panaro river	5.6	-	-	-	-
S9	S9-1M	gypsum	G1	-	-	-	-	-	0.5	6.5	1.5
	S9-4M Tirelli et al. 2020	lime	2	1.5	very fine-medium, moderately sorted	Panaro river	3.4	-	-	7.6	-

Table 2 Petrographic characteristics of mortars.

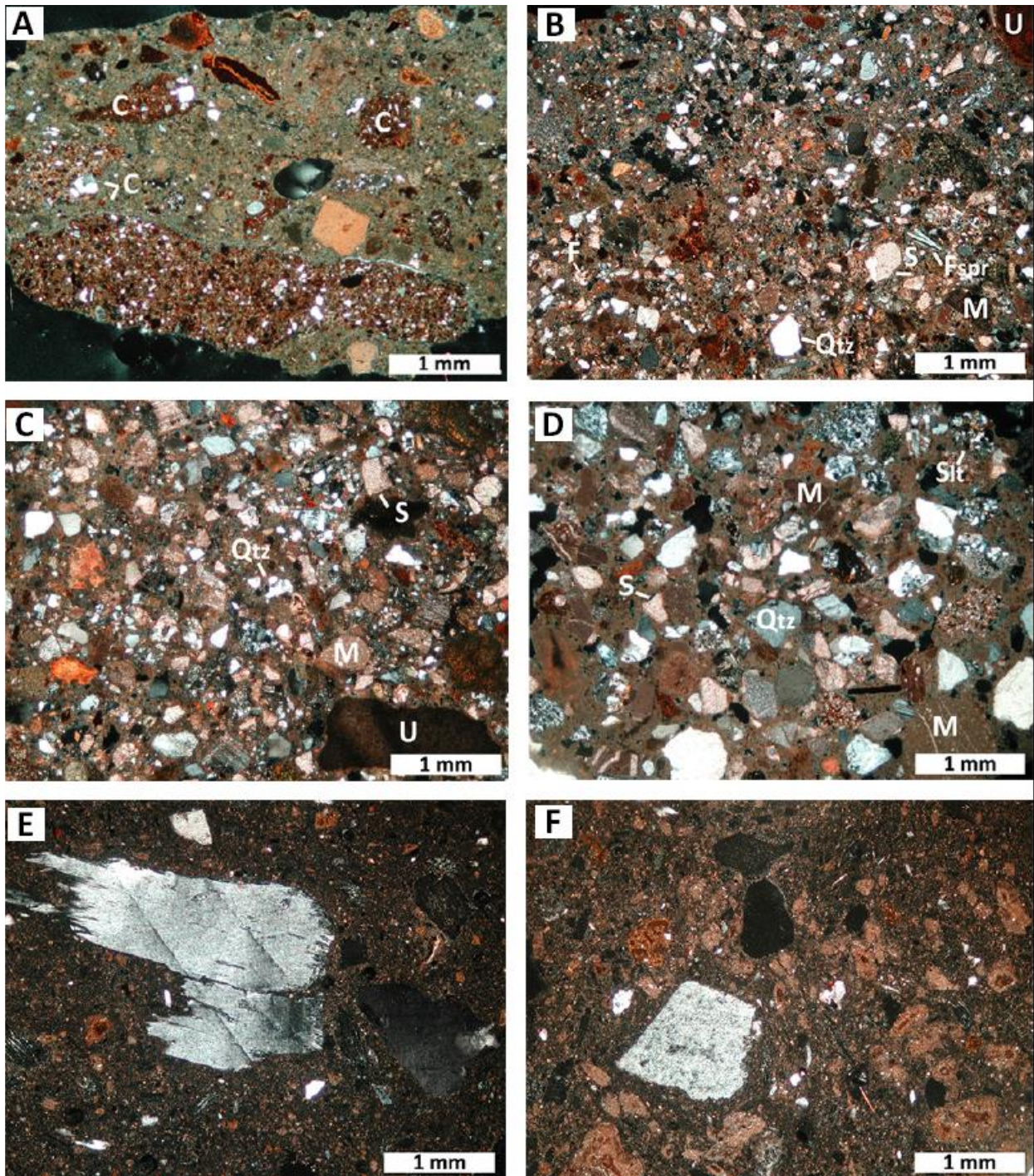


Fig. 3 A) photomicrograph of group 1 mortar (sample C2-3M, crossed polars); c: cocchiopesto fragments; B) photomicrograph of group 2 mortar (sample C1-1M, crossed polars). f: fossil fragment, Fspr: feldspar, m: micritic limestone, Qtz: quartz, s: sparry calcite, u: underburned fragment; C) photomicrograph of group 3 mortar (sample N9-3M, crossed polars). m: micritic limestone, Qtz: quartz, s: sparry calcite, u: underburned fragment; D) photomicrograph in of group 4 mortar (sample N3-2AM, crossed polars). m: micritic limestone, Qtz: quartz, Slf: siltstone fragment; E) photomicrograph in of gypsum mortar G1 (sample C5-6M, crossed polars), showing a large selenite fragment in the gypsum groundmass (center-left); F) photomicrograph of gypsum mortar G2 (sample C5-7M, crossed polars) characterized by abundant fragments of micritic carbonate rock and shale; a selenite fragment is visible at center left (grey).

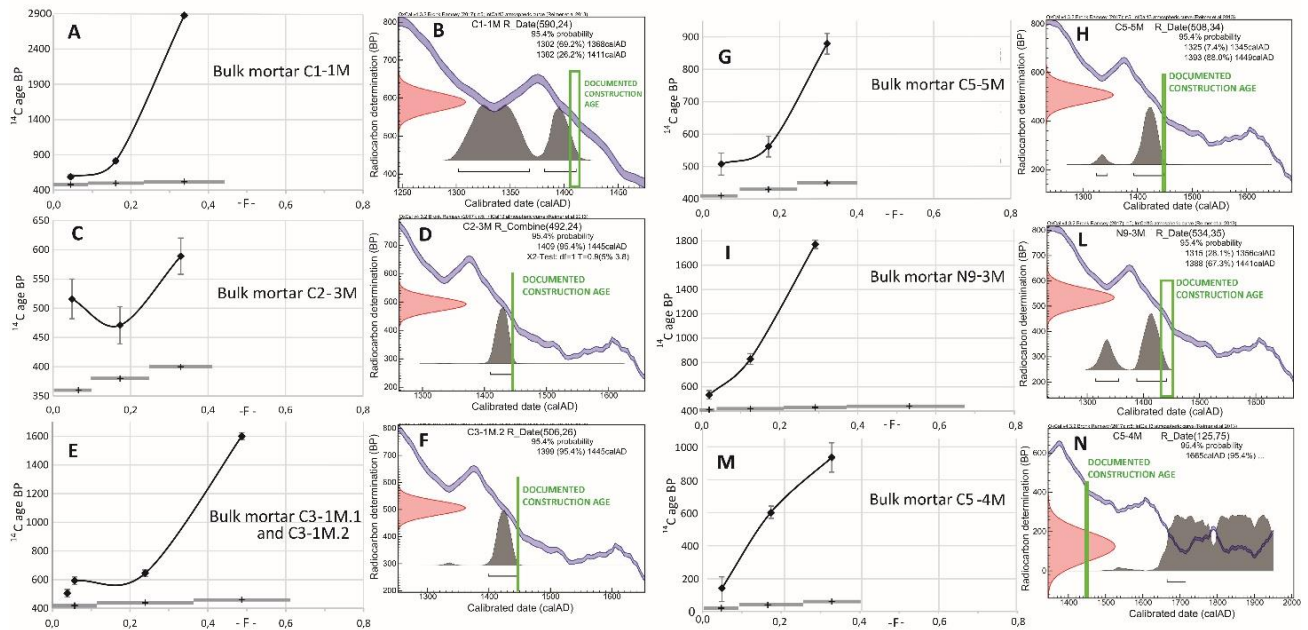


Fig. 4 ^{14}C age profiles and calibrated calendar ages for the lime mortars from the 15th century vaults in the Modena cathedral. The construction time spans inferred from historical documents for each single vault are marked by green boxes.

Sample	Vault	Sample type	Building age (Baracchi 1993)	Dating method	Date	Notes	Pollen markers	Interpretation
C1-1M	C1	lime mortar group 2	1404-1415	¹⁴ C ETH Zurigo	1302-1368 (69.2%) 1382-1411 (26.2%)	date in AGREEMENT with building age		Lime mortar for original construction and for later repair after the 1660 or 1671 earthquake
C1-1L	C1	brick in lime mortar (not sampled)		TL UniMiBi	1640 ± 40	later repair		
C2-3M	C2	lime mortar group 1	1443-1445	¹⁴ C ETH Zurigo	1409-1445 (95.4%)	date in AGREEMENT with building age		lime mortar for original construction
C3-1M	C2	lime mortar group 1	1446-1447?	¹⁴ C ETH Zurigo	1399-1445 (95.4%)	date in AGREEMENT with building age		lime mortar for original construction with new bricks
C3-1L	C3	brick in lime mortar C3-1M		TL UniMiBi	1500 ± 60	date in AGREEMENT with building age		
C5-1L	C5	brick in lime mortar C5-1M	1447?-1453	TL UniMiBi	1280 ± 65	RE-USED bricks		Lime mortars for original construction with re-used bricks. Gypsum mortar G1 for repair with re- used bricks and gypsum mortar G2 for later repair after the 1850 or 1832 earthquake
C5-4L	C5	brick in lime mortar C5-4M		TL UniMiBi	1320 ± 65	RE-USED bricks		
C5-5M	C5	lime mortar group 1		¹⁴ C ETH Zurigo	1325-1345 (7.4%) 1393-1449 (88.0%)	date in AGREEMENT with building age		
C5-5L	C5	brick in lime mortar C5-5M		TL UniMiBi	225 ± 170	RE-USED bricks		
C5-6L	C5	brick in gypsum mortar G1		TL UniMiBi	250 ± 170	RE-USED bricks	<i>Cannabis sativa</i> in gypsum mortar G1	
C5-7L	C5	brick in gypsum mortar G2		TL UniMiBi	1835 ± 20	later repair	<i>Cannabis sativa</i> in gypsum mortar G2	
N3-3ALa	N3	brick in gypsum mortar G1	?	TL UniMiBi	1820 ± 20	later repair	<i>Ginkgo biloba</i> , <i>Cedrus</i> , <i>Cannabis sativa</i> in gypsum mortar G1	Gypsum mortar for later repair after the 1811, 1832 or 1850 earthquake
N3-3ALb	N3	brick in gypsum mortar G1		TL UniMiBi	1840 ± 20			
N8-1L	N8	brick in lime mortar N8-1M	1433-1454	TL UniMiBi	1050 ± 90	RE-USED bricks		Lime mortar for later repair with re- used bricks after the 1501, 1505, 1586, 1660 or 1671 earthquake. Gypsum mortar for later repair after earthquake the 1811 (Tirelli et al. 2020)
N8-1M	N8	lime mortar group 3		¹⁴ C Aarhus AMS Centre	1487-1681 (79.2%) 1739-1743 (0.4%) 1763-1802 (12.4%) >1938 (3.5%)	date YOUNGER than building age: later repair		
N8-2Lc	N8	brick in gypsum mortar G1		TL UniMiBi	1740 ± 20	later repair	<i>Ginkgo biloba</i> , <i>Allanthus altissima</i> in gypsum mortar G1	
N8-2La	N8	brick in gypsum mortar G1		TL UniMiBi	1740 ± 30			
N8-2Lb	N8	brick in gypsum mortar G1		TL UniMiBi	1805 ± 20			
N9-1L	N9	brick in gypsum mortar G1	1433-1454	TL UniMiBi	1330 ± 75	RE-USED bricks		Lime mortar for original construction with re-used bricks. Gypsum mortar for later repair with re-used bricks
N9-3M	N9	lime mortar group 3		¹⁴ C Aarhus AMS Centre	1315-1356 (28.1%) 1388-1441 (67.3%)	date in AGREEMENT with building age		
N9-3L	N9	brick in lime mortar N9-3M		TL UniMiBi	1340 ± 70	RE-USED bricks		
S9-1La	S9	brick in gypsum mortar G1	1404-1433	TL UniMiBi	1235 ± 80	RE-USED bricks	<i>Cannabis sativa</i> in gypsum mortar G1	Lime mortar for original construction with re-used bricks. Gypsum mortar for later repair with re-used bricks (Tirelli et al. 2020)
S9-1Lb	S9	brick in gypsum mortar G1		TL UniMiBi	1250 ± 80	RE-USED bricks		
S9-4M	S9	lime mortar group 2		¹⁴ C ETH Zurigo	1328-1341 (5.2%) 1396-1439 (90.2%)	date in AGREEMENT with building age	<i>Cannabis sativa</i> in lime mortar group 2	
S9-4L	S9	brick in lime mortar S9-4M		TL UniMiBi	1245 ± 65	RE-USED bricks		

Table 3: absolute dating results and interpretation. Reported are also the preliminary results of vaults N8 and S9 from Tirelli et al., 2020. UniMiBi: Università Milano-Bicocca.

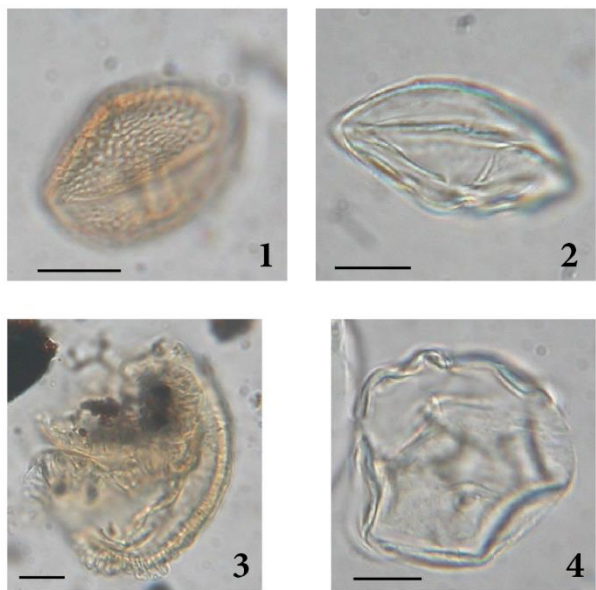


Fig. 5 Pollen from the vault mortars seen under the optical microscope: 1) *Ailanthus altissima* (sample N8-2M); 2) *Ginkgo biloba* (sample N8-2M); 3) *Cedrus* (sample N3-3AM); 4) *Cannabis sativa* (sample S9-1M). Scale bar is 10 μ m.

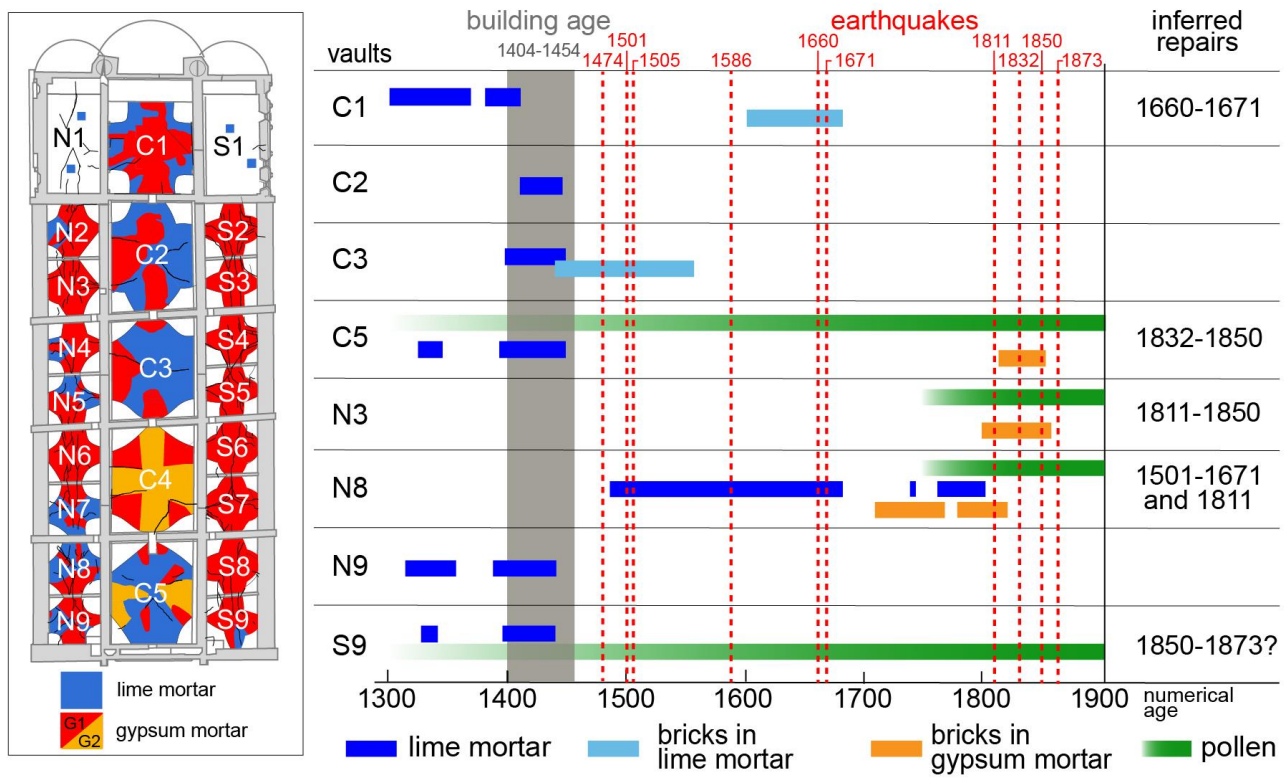


Fig. 6: Time lines of damaging earthquakes and results of ^{14}C and TL absolute dating and pollen analysis for the vaults construction materials (first appearance *Ginkgo biloba* and *Ailanthus altissima* in vaults N3 and N9; increase in *Cannabis sativa* for vaults C5 and S9).